Journal of Sound and Vibration (1973) **28**(1), 1–13

ACOUSTIC RADIATION FROM THE END OF A TWO-DIMENSIONAL DUCT, EFFECTS OF UNIFORM FLOW AND DUCT LINING

S. M. CANDEL
Daniel and Florence Guggenheim Jet Propulsion Center,
Kármán Laboratory of Fluid Mechanics and Jet Propulsion,
California Institute of Technology,
Pasadena, California 91109, *U.S.A.*

(*Received* 18 *September* 1972)

A study is presented of the radiation of acoustic modes from the end of a duct immersed in a uniformly moving medium. It is shown that the uniform flow has roughly the same effect as an increase in frequency at constant mode number: the number of lobes of the radiation pattern increases, and the radiation maximum is slightly displaced towards the duct axis. When the mode is near cut-off the forward radiation for an inlet is enhanced. The acoustic radiation characteristics of ducts with soft or absorbing walls and hard, perfectly-reflecting walls are then compared. It is shown, and this is of technological interest, that the side radiation from the end of an acoustically soft duct is greatly reduced for lower-order modes.

1. INTRODUCTION

The present-day trend is to design and use high-bypass turbofan engines as power plants for subsonic aircraft. The dominant noise source in these engines is associated with the turbomachinery. The fan, in particular, which is the largest element, displaces the greatest amount of air and is most exposed to ground observation, is a strong noise generator. The noise produced consists of three types: discrete tones generated by rotor blade passage and impingement of wakes on the stator vanes, multiple pure tones at lower frequencies associated with rotating shock patterns, and broadband noise. The fan noise is essentially coherent and composed of discrete tones; even the "broadband noise" has been identified by Mather *et al.* [1] as a series of close discrete tones propagating as plane waves, produced by the rotation at shaft frequency of pressure field non-uniformities existing in each blade channel.

The pure tones produced at the blade passage frequency and its harmonics are prominent in present-day engines, with pressure levels reaching 160 dB in the inlet and exhaust ducts and frequencies situated in the range (2000 to 7000 Hz) of greatest sensitivity for the human ear [2]. Tyler and Sofrin [3] described elegantly the generation, propagation, and radiation of these pure tones and showed in particular how the rotor and stator interact to excite propagating duct modes.

An important aspect of the transmission of sound generated by a turbofan is the radiation from the duct end sections into the surrounding space. The angular distribution of acoustic energy directly influences the sound pressure level at various positions with respect to the aircraft and is of particular importance on the ground and on the sideline. The distribution of radiated energy depends on the duct geometry, the acoustic characteristics of the propagating mode, the internal and external flow conditions (mean velocities and sound speeds), and on the surface quality near the duct edges.

In connection with aircraft engine noise the radiation problem has received relatively little recent discussion in the literature, in contrast with the large amount of work devoted to the propagation characteristics of the duct modes. The possibility of changing the radiation pattern by modifying the aperture field (i.e., by modifying the energy-carrying modes) has received little attention. The attenuation properties of acoustical lining have been extensively studied, but its effect on the external radiation also seems to have been overlooked. In usual practice, the distribution pattern of energy is computed by replacing the duct by an infinite wall with an aperture, neglecting the flow presence, and applying the Fraunhofer approximation of optics (see, for example, reference [3]).

The purpose of this paper is to describe a study of the acoustic radiation from a duct immersed in a uniform flow and then to discuss some features of the acoustic radiation from a duct lined with sound-absorbing material. The limiting case when the walls are ideally soft is considered for simplicity, and provides an upper bound to the effects one can expect to obtain by installation of absorbing material on the duct walls. It is shown that the side radiation from a lined duct can be greatly reduced, which is a result of technological interest.

Analysis of the uniform flow situation is appropriate here because it approximates the flow condition at the engine inlet. At the fan exhaust, the flow becomes nearly uniform when the aircraft and exhaust gases have the same velocity (this is the case a few miles after take-off or before landing under reduced power operation).

When the engine is tested on the ground, or during the initial moments of take-off, a large velocity difference exists between the exhaust gases and the atmosphere, and sound waves radiated by the engine are deflected sideways. This situation has been recently investigated by Mani [4]. Mani considered a rectangular duct containing a uniform flow discharging in a stationary atmosphere. Using the Wiener–Hopf technique and an approximate solution he obtained the far field pressure distribution. If, in addition, the outer atmosphere is colder than the jet core, Candel [5] has shown that the deflection of the transmitted waves is enhanced. For a hot core like the primary exhaust jet, the maximum radiation occurs at large angles, 60 to 70 degrees from the jet axis. In these situations, refraction effects are of great importance.

In the present work velocity and temperature discontinuities are not considered. The duct radiates into a uniform subsonic flow. The solution may be obtained by applying a simple transformation to the known solution of an associated radiation problem in a stationary medium. The method is quite similar to that used in reference [6] to study the diffraction of plane waves by a half plane immersed in a uniform flow. It is appropriate to start by formulating the radiation problem in a stationary medium.

2. ANALYSIS OF THE PROBLEM

2.1. RADIATION PROBLEM IN A STATIONARY MEDIUM

Consider a semi-infinite cylindrical duct parallel to the x-axis, its end section at $x = 0$, normal to the x-axis. Suppose for the moment that the duct has hard (or perfectly reflecting) walls.

Because the medium is stationary, the pressure perturbation and velocity potential may be used interchangeably to describe the boundary value problem. The problems will be stated in terms of a general potential ϕ^0.

All the waves are of the form $\phi^0 \exp(-i\omega t)$ where ϕ^0 satisfies the following boundary value problem:

$$\phi^0_{xx} + \phi^0_{yy} + \phi^0_{zz} + k^2 \phi^0 = 0, \tag{1}$$

$$\frac{\partial \phi^0}{\partial n} = 0 \tag{2}$$

on the cylinder surface, where $k = \omega/c$.

The boundary condition (2) expresses that the displacement vanishes at the hard wall. To express a radiation problem for a particular mode propagating in the duct, the complete field ϕ_c^0 is decomposed into an incoming wave ϕ_i^0 traveling along the duct in the positive x-direction and a field ϕ^0 induced by the incoming wave when it radiates from the duct:

$$\phi_c^0 = \phi_i^0 + \phi^0. \tag{3}$$

The complete field ϕ_c^0 must satisfy one of the edge conditions

$$\phi_c^0[x, R_+(\theta), \theta] - \phi_c^0[x, R_-(\theta), \theta] \sim x^{1/2} \tag{4}$$

as $x \to 0_-$ on the duct surface, or

$$\frac{\partial \phi_c^0}{\partial y} \sim x^{-1/2} \tag{5}$$

as $x \to 0_+$ on the duct continuation.

Condition (4) represents the behavior of the pressure jump for an incompressible flow near a trailing edge, while condition (5) applies to the velocity potential near a leading edge. For the stationary medium under consideration, the pressure and velocity potentials are proportional, and both conditions (4) and (5) lead to the same solution.

In addition to equations (1) and (2), and the edge conditions (4) and (5), the function ϕ^0 must satisfy Sommerfeld's radiation condition at infinity:

$$\lim_{r\to\infty} r\left(\frac{\partial \phi_c^0}{\partial r} - ik\phi_c^0\right) = 0. \tag{6}$$

(Here r is the radial coordinate of a spherical polar coordinate system (r, θ, ϕ).)

Suppose that one duct mode has been excited far upstream in the duct and propagates in the positive x-direction towards the duct end. This mode constitutes the incoming wave with a potential of the form

$$\phi_i^0 = e^{ik_x x} f(y, z). \tag{7}$$

This potential satisfies equations (1) and (2); thus, $f(y,z)$ is an eigenfunction of the problem

$$f_{yy} + f_{zz} + \mu^2 f = 0, \tag{8}$$

$$\frac{\partial f}{\partial n} = 0 \tag{9}$$

on the duct surface, where μ is defined by

$$\mu^2 = k^2 - k_x^2. \tag{10}$$

Non-trivial solutions of the problem specified by equations (8) and (9) occur only for the eigenvalues μ_{mn} of μ. Of interest here is the case in which the incoming wave is a propagating mode: that is, a mode with a real wave number k_x. From equation (10),

$$k_x = k[1 - (\mu/k)^2]^{1/2}, \tag{11}$$

so that k_x will be real if $\mu^2 < k^2$. The factor $[1 - (\mu/k)^2]^{1/2}$ appears very often and is therefore given a specific symbol,

$$\eta = [1 - (\mu/k)^2]^{1/2}. \tag{12}$$

The preceding formulation applies to any cylindrical geometry. However, the radiation problem has been solved exactly for a few cases only. To discuss the effects of free stream and wall absorption a reliable computation scheme is needed for the radiation patterns in a stationary medium. It is convenient to consider a duct formed by two parallel, semi-infinite plates (Figure 1(a)); an exact solution for the radiation from the duct may be obtained by the Wiener–Hopf technique and is elegantly described by Noble [7, see pp. 105–110]. This solution is easily arranged in computable form (details may be found in references [8] or [4]).

To study the radiation from a jet engine, it would be more appropriate to consider the radiation from an annular duct. However, the exact solution for this geometry is complicated; moreover, an approximate relationship exists between the annular duct and the two plate duct modes, and consequently between the corresponding radiation patterns (Appendix I).

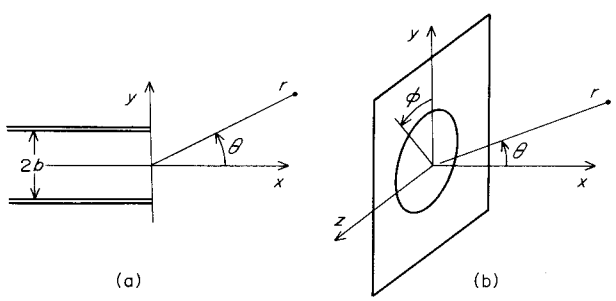

Figure 1. Sketches showing geometry of (a) a two plate duct and (b) a cylindrical duct aperture.

Radiation patterns are most generally computed by an approximate method described in reference [8]. The procedure employed replaces the duct by a plane screen with an aperture (Figure 1(b)) and the Fraunhofer approximation is applied. This leads to a simple relation between the *far field radiation* and the *Fourier transform of the field* in the aperture. This method may therefore be applied to any cylindrical geometry for which the Wiener–Hopf solution is intractable, and provides a useful tool for analytical study of the influence on the radiation pattern of a change in the aperture field.

For the two plate duct of Figure 1(a), an incoming wave of amplitude A has the form

$$p_i = A\, e^{ik_x x} \cos \mu_N (y - b), \tag{13}$$

where

$$\mu_N = N\pi/2kb. \tag{14}$$

The pressure far field outside the duct has the form

$$p_c \sim A h_0(\theta; kb, N)(b/r)^{1/2}. \tag{15}$$

(Here r is the radial coordinate of a cylindrical coordinate system (r, θ).) The *pressure angular distribution* $h(\theta; kb, N)$ is dimensionless, of order one, and depends only on the reduced frequency $kb = \omega b/c$, the mode number N, and the Mach number M when a uniform flow is present.

Also

$$D(\theta; kb, N) = 20 \log_{10} h_0(\theta; kb, N) \tag{16}$$

is the value of h_0 in decibels. The sound pressure level in the far field may be deduced from equation (15) and definition (16):

$$\text{SPL} = \text{SPL(duct)} + D(\theta; kb, N) + 10 \log_{10}(b/r). \tag{17}$$

By using both exact and approximate techniques, $D(\theta; kb, N)$ has been calculated for several values of kb and N. A few typical patterns are shown on Figures 2(a)–(c), $M = 0$. The two techniques yield very similar patterns, both in amplitude and angular distribution. Large differences occur near cut-off (when $N\pi/2kb$ approaches one), in particular in the neighborhood of the normal to the duct axis. This is to be expected because the duct is replaced in the approximate method by an infinite screen that lies in this plane (Figure 1(b)).

The difference between exact and approximate pressure fields may reach 7 dB, but remains in general small, and the approximate method may be used with confidence for other cylindrical geometries (except near cut-off and in the neighborhood of the normal direction).

2.2. RADIATION PROBLEM FOR A CYLINDRICAL DUCT IMMERSED IN A SUBSONIC UNIFORM FLOW

It was noted in reference [6] that an essential difference exists between positive (exhaust) and negative (inlet) flow directions. In the first case, the duct has a trailing edge, the Kutta–Joukowski condition applies, the pressure jump satisfies the edge condition (4), and the pressure is continuous across the duct continuation. In the second case, the duct wall has a leading edge, the velocity potential satisfies condition (5) and is continuous in the upstream region.

One can proceed as in reference [6] by describing the general problem by using a function ϕ which represents the pressure perturbation p when $M > 0$ and the velocity potential ϕ when $M < 0$.

All the waves are now solutions of the convective wave equation

$$\phi_{xx}(1 - M^2) + \phi_{yy} + \phi_{zz} + 2Mik\phi_x + k^2\phi = 0 \tag{18}$$

and satisfy the condition of vanishing displacement at the hard wall:

$$\frac{\partial \phi}{\partial n} = 0. \tag{19}$$

The complete field ϕ_c satisfies one of the edge conditions (4) or (5) and Sommerfeld's radiation condition (6) at infinity. The incoming wave ϕ_i has the form (7) where $f(y,z)$ is an eigenfunction of the boundary value problem specified by equations (8) and (9), but in the present situation ϕ_i satisfies the convective wave equation (18) and the expression for k_x is modified:

$$k_x = \frac{k}{(1 - M^2)}\left[1 - \left(\frac{\mu}{k}\right)^2 (1 - M^2)\right]^{1/2} - \frac{kM}{1 - M^2}. \tag{20}$$

It is convenient to make the following definitions [6]:

$$k_1 = k/(1 - M^2)^{1/2}, \tag{21}$$

$$x_1 = x/(1 - M^2)^{1/2}, \tag{22}$$

$$\psi(x_1, y; k_1, \mu) = e^{ik_1 M x_1}\, \phi(x, y; \mu, M). \tag{23}$$

The function ψ is the solution of the boundary value problem specified by equations (1), (2), (4) (or (5)), and (6), where x is replaced by x_1 and k by k_1.

The incoming wave potential has the form

$$\psi_i = e^{ik_1\eta_1 x_1} f(y, z), \tag{24}$$

where

$$\eta_1 = [1 - (\mu/k_1)^2]^{1/2}. \tag{25}$$

The radiation problem for ψ is completely identical to an associated radiation problem in a stationary medium and hence one can write

$$\psi = \phi^0(x_1, y; k_1, \mu); \tag{26}$$

then, from equation (23), the complete field is

$$\phi_c(x, y; k, \mu, M) = e^{-ik_1 M x_1} \phi_c^0(x_1, y; k_1, \mu). \tag{27}$$

Thus, the complete field corresponding to an incoming wave (k, μ) in the uniform flow case may be obtained from the complete field for an associated radiation problem in a stationary medium for an incoming wave (k_1, μ) and a stretched x coordinate, x_1.

When $1 > M \geqslant 0$, then, from the definition of ϕ and relation (27),

$$p_c(x, y; k, M, \mu) = e^{-ik_1 M x_1} \phi_c^0(x_1, y; k_1, \mu). \tag{28}$$

When $-1 < M \leqslant 0$, ϕ represents the velocity potential φ and the pressure perturbation may be found through the relation

$$p_c = -\bar{\rho}\left(-i\omega\varphi_c + \bar{u}\frac{\partial \varphi_c}{\partial x}\right). \tag{29}$$

Using equations (27) and (29), and dividing by the amplitude of the incoming pressure wave, yields the complete pressure field associated with a duct pressure mode of amplitude unity:

$$p_c = \frac{1}{1 - M\eta_1}\left[\phi_c^0 + \left(\frac{iM}{k_1}\right)\frac{\partial \phi_c^0}{\partial x_1}\right] e^{-ik_1 M x_1}. \tag{30}$$

This expression is not convenient because both ϕ_c^0 and $\partial\phi_c^0/\partial x_1$ appear. To proceed, an actual expression for ϕ_c^0 has to be inserted in equation (30). Generally, ϕ_c^0 appears in integral form (for instance, for the two plate duct, ϕ_c^0 is given by Noble [7, see equations (3.34) and (3.37)]). Applying equation (30) to this form and using the saddle point method yields

$$p_c \sim \frac{1 - M\cos\theta_1}{1 - M\eta_1}\phi_c^0(x_1, y; k_1, \mu) e^{-ik_1 M x_1}, \tag{31}$$

where (r_1, θ_1) are the polar coordinates corresponding to the Cartesian coordinates (x_1, y) and related to (r, θ) by

$$\tan\theta_1 = (1 - M^2)^{1/2}\tan\theta, \tag{32}$$

$$r_1 = r\left(\frac{1 - M^2}{1 - M^2\sin^2\theta}\right)^{1/2}. \tag{33}$$

For the negative flow direction, the pressure field contains an additional multiplying factor

$$(1 - M\cos\theta_1)/(1 - M\eta_1). \tag{34}$$

This factor is of order one, being larger than one when $\theta_1 < \arccos\eta_1$: i.e., when

$$\theta < \arccos\left[(1 - M^2)^{1/2}\eta_1/(1 - M^2\eta_1^2)^{1/2}\right]. \tag{35}$$

Factor (34) becomes important near cut-off when η_1 is near zero. The forward radiation is then enhanced by 0 to 5 dB.

From expressions (28) and (31), the relations between the angular distribution $h_0(\theta; k, \mu)$ for a stationary medium and $h(\theta; k, \mu, M)$ for a moving medium can be deduced. When $1 \geqslant M > 0$,

$$h(\theta; k, \mu, M) = \left(\frac{1 - M^2}{1 - M^2\sin^2\theta}\right)^{1/4} h_0(\theta_1; k_1, \mu). \tag{36}$$

When $-1 \leqslant M < 0$,

$$h(\theta; k, \mu, M) = \frac{1 - M\cos\theta_1}{1 - M\eta_1}\left(\frac{1 - M^2}{1 - M^2\sin^2\theta}\right)^{1/4} h_0(\theta_1; k_1, \mu). \tag{37}$$

For radiation in three dimensions, the exponent 1/4 of equations (36) and (37) should be replaced by 1/2.

3. RESULTS

Before proceeding to the discussion, it is worth giving some of the characteristics of the discrete tone noise generated by a typical turbofan. The noise of a JT3D-3B Pratt and Whitney engine is described in some detail by Marsh *et al.* [2]. The sound pressure level in the JT3D reaches 150 to 160 dB (620 to 2000 N/m^2) in the inlet and exhaust ducts. The fundamental frequencies lie between 1800 and 3700 Hz. A complete noise spectrum may be found in reference [2] (see Figure 16).

The inlet duct radius is approximately $r_0 \simeq 0{\cdot}62$ m and so $kr_0 \simeq 35$. Little information is available concerning the type of mode which carries the acoustic energy; however, the radial mode number remains generally low. According to Appendix I, the parameter kb should be selected below 35 and the mode number N below 5 or 6.

A number of radiation patterns have been computed; some typical examples are shown in Figures 2(a)–(c). The effect of the uniform flow has been included both for an inlet $M < 0$ and exhaust situation $M > 0$.

When the reduced frequency kb is increased, the radiation patterns show a larger number of lobes, a greater peak pressure, and more energy is radiated near the duct axis.

At constant frequency, an increase in the mode number N results in a greater side radiation. The angle of maximum radiation rotates away from the jet axis. By using ray acoustics it can be shown that for a stationary medium the direction of maximum radiation has a polar angle approximately given by

$$\cos\theta_{\max} \simeq \eta. \tag{38}$$

When the duct radiates in a uniformly moving medium, relation (38) may be transformed according to equation (32) and yields

$$\cos\theta_{\max} \simeq (1 - M^2)^{1/2}\eta_1/(1 - M^2\eta_1^2)^{1/2}. \tag{39}$$

The right-hand side of expression (39) depends very weakly on the Mach number and the position of the maximum of radiation remains very near to its position in a stationary medium. This appears clearly on Figures 2(a)–(c).

This result is in sharp contrast with the situation where the duct discharges a hot jet of Mach number M in a cold atmosphere. In that case, the angle of maximum radiation deduced from ray acoustics is given by

$$\cos\theta_{\max} \simeq (c_2/c_1)\eta_1/(1 + M\eta_1), \tag{40}$$

where c_1 and c_2 are the sound speeds in the jet and the atmosphere. For the radiation from a primary exhaust duct this angle is about 70° (see reference [5]).

The preceding discussion shows that for a given frequency and amplitude it is desirable to have lower-order modes radiating from an engine duct. For a low value of $N\pi/2kb$ (more generally, μ_{mn}/k), the maximum of radiation is near the duct axis and the side radiation is reduced, a uniform flow slightly accentuating these features.

In the next section it will be shown that acoustical lining inserted in the engine duct most effectively cuts side radiation for low values of $N\pi/2kb$. This shows the importance of knowing

what type of mode transports the acoustic energy and singles out the lower order modes as more desirable.

The presence of a uniform flow has roughly the same effect as an increase in frequency at constant mode number. Most visible is the increase in the number of lobes; this number is determined as the largest integer contained in $k_1 b/\pi$. The radiation is slightly more efficient and the amplitude is mostly affected near the duct axis.

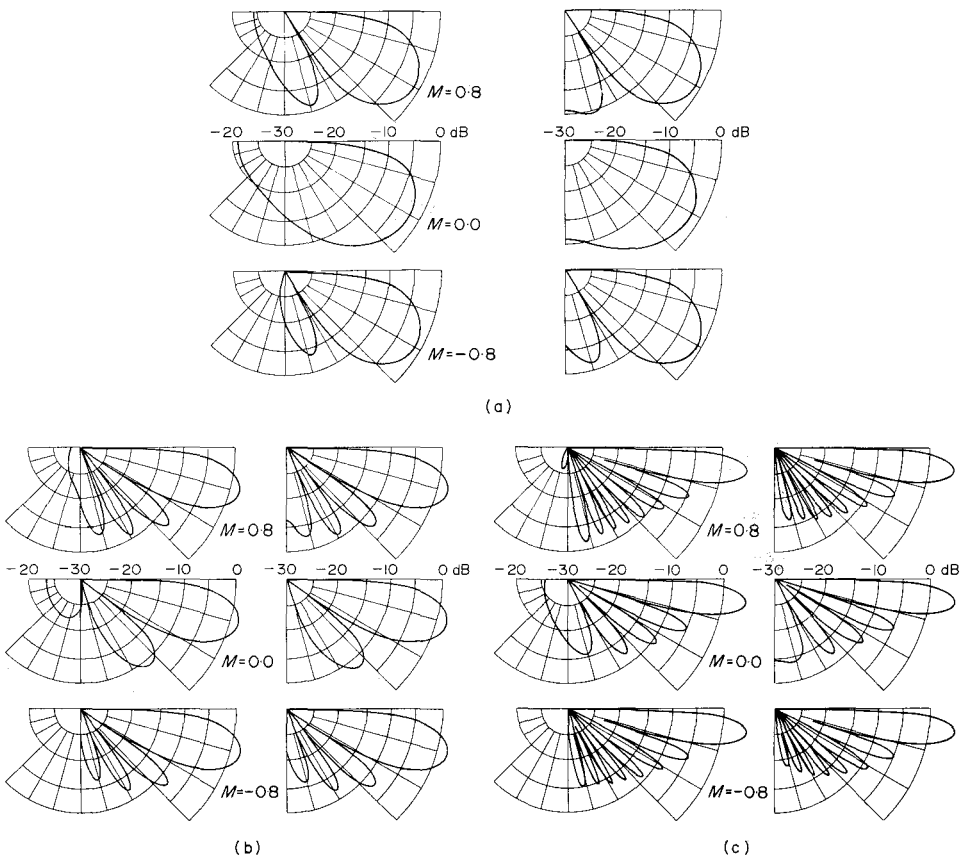

Figure 2. Radiation patterns $D(\theta; kb, N, M)$ for a hard wall duct at selected Mach numbers (M). Left figures: the exact Wiener Hopf solution. Right figures: the approximate Fraunhofer solution. (a) $kb = 4$, $N = 1$; (b) $kb = 8$, $N = 1$; (c) $kb = 16$, $N = 1$.

To see this more clearly, it is easy to obtain a full analytical expression for the angular distribution $h(\theta; k, \mu, M)$ by using the results of reference [8]. Consider, for example, N even and different from zero and M positive; then

$$h(\theta; k, \mu, M) = Qg(\theta), \tag{41}$$

where Q is an amplitude,

$$Q = (2\pi)^{-1/2}(k_1 b)^{1/2}\eta_1[(1 - M^2)/(1 - M^2 \sin^2\theta)]^{1/4}, \tag{42}$$

and $g(\theta)$ is a normalized angular function,

$$g(\theta) = \frac{(2/k_1 b)\sin\theta_1 \sin(k_1 b \sin\theta_1)}{(\mu N/k_1)^2 - \sin^2\theta_1}, \tag{43}$$

such that for the approximate value of θ_{max},

$$g(\theta_{max}) = 1.$$

If Q is compared to Q_0 (corresponding to $M = 0$),

$$\frac{Q}{Q_0} = \frac{\eta_1}{\eta}(1 - M^2 \sin^2\theta)^{-1/4}, \tag{44}$$

and thus Q shows a weak dependence on M and is mostly affected for θ near 90°. In the expression for $g(\theta)$ the polar angle θ_1 replaces θ and the reduced frequency increases from kb to $k_1 b$, which explains the increase in the number of lobes of the radiation patterns.

4. SEMI-INFINITE DUCT WITH ABSORBING WALLS

While noise attenuation properties of acoustic lining set on the duct walls have been studied extensively, its effect on the radiation pattern has been overlooked.

The presence of acoustical lining on a duct wall is usually described by an impedance relation between the pressure and normal velocity fluctuations on the lining surface. If $Z_A = R_A + iX_A$ is the acoustic impedance of the lining, its specific acoustic impedance is the value of Z_A normalized by the characteristic impedance of air:

$$\zeta = Z_A/\rho c = (R_A/\rho c) + i(X_A/\rho c); \tag{45}$$

the specific admittance is defined as the inverse of ζ:

$$\beta = 1/\zeta. \tag{46}$$

The condition on the wall becomes, when the medium is stationary,

$$\frac{\partial p}{\partial n} = ik\beta p. \tag{47}$$

An acoustically hard (or perfectly reflecting) wall has a vanishing admittance. An ideally soft wall has an infinite admittance; realizable linings have finite, simultaneously resistive and reactive, admittances.

Because of condition (47), the duct modes are exponentially attenuated along the duct, their radial distribution $f(y,z)$ is modified, and the associated radiated field changes.

Another more physical description is as follows. The absorbing walls focus the acoustic energy towards the center of the duct, while near the walls the energy is absorbed and the pressure fluctuation reduced. The amplitude of the pressure field in the aperture decreases towards the edges. This is equivalent to a reduction of the aperture area and would result in a broader main lobe in the radiation pattern and thus a lower directionality. However, the radial decrease in pressure amplitude also produces a large reduction in the side lobe amplitudes. Such phenomena are well known in the theory of aperture antennas (see, for instance, the discussion by Collin [10, p. 76]).

The effects described above may be shown simply by considering the radiation from a duct with perfectly soft walls ($\beta = \infty$, the pressure fluctuation vanishes on the duct wall). Consider this situation for a duct of Figure 1(a). The pressure amplitude in the far field is given in reference [8], for incoming duct modes of the form

$$p_1 = e^{ik_x x} \sin \mu_N (y - b),$$

where $\mu_N = N\pi/2kb$.

The eigenvalues μ_N and the wavenumbers in the x-direction are unchanged from their respective values in the hard-walled case, but the eigenfunctions satisfy the new boundary condition and vanish on the plates.

The effect of a uniform flow may be included without effort by applying the transformation of section 2. This is possible because the new condition at the wall, $\phi_c = 0$, and the new condition near the edge, $\phi[x, R(\theta), \theta] \to C_1$ as $x \to 0_+$ on the duct continuation, do not essentially affect the argument given in section 2.

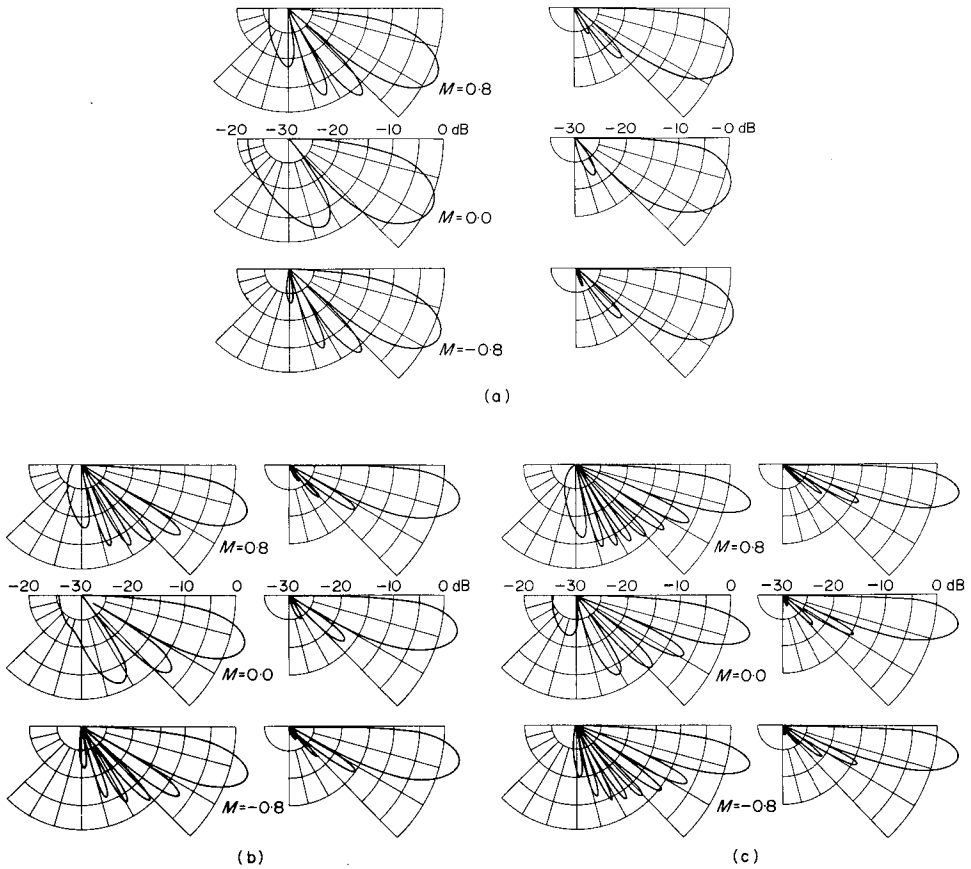

Figure 3. Radiation patterns $D(\theta; kb, N, M)$ for $N = 2$ modes in a hard wall duct (left side figures) and a soft wall duct (right side figures), for selected Mach numbers (M) and duct width parameters (kb). (a) $kb = 8$; (b) $kb = 12$; (c) $kb = 16$. $M < 0$: inlet radiation; $M < 0$: exhaust radiation.

A few radiation patterns for $N = 2$ modes propagating in the "soft wall" duct are shown on the right sides of Figures 3(a)–(c). On the left sides, the radiation patterns for a hard wall duct are given for comparison. The side radiation from the soft duct is very weak (generally 20 dB between the main lobe and the first side lobe); the main lobe as predicted is slightly wider.

The ideally soft duct has an infinite admittance which is not modified by the uniform flow in the duct. Consequently, the uniform flow only slightly changes the radiation patterns; the number of side lobes increases, but their amplitude is very small and the patterns appear almost unchanged.

The ratio between the far field pressures corresponding to soft and hard ducts is derived in reference [8] and reproduced here; it is

$$\tau = |p_{\text{soft}}|/|p_{\text{hard}}| = (N\pi/2kb)(1 + \eta)^{-1} \cot(\theta/2), \tag{48}$$

and is represented graphically on Figure 4 for $N = 1$ and $N = 2$. The reduction in side radiation appears clearly when $(N\pi/2kb)$ is sufficiently small.

It is interesting at this point to make a small digression and compare the diffracted fields for a plane wave (k, Θ) incident, respectively, on a hard and on a soft edge. The incident wave has a potential of the form

$$\phi_i = \exp(-ikx\cos\Theta - iky\sin\Theta). \tag{49}$$

Here only the asymptotic expressions for the diffracted fields valid for $kr \gg 1$ and θ far from $\pm(\pi - \Theta)$ need be given.

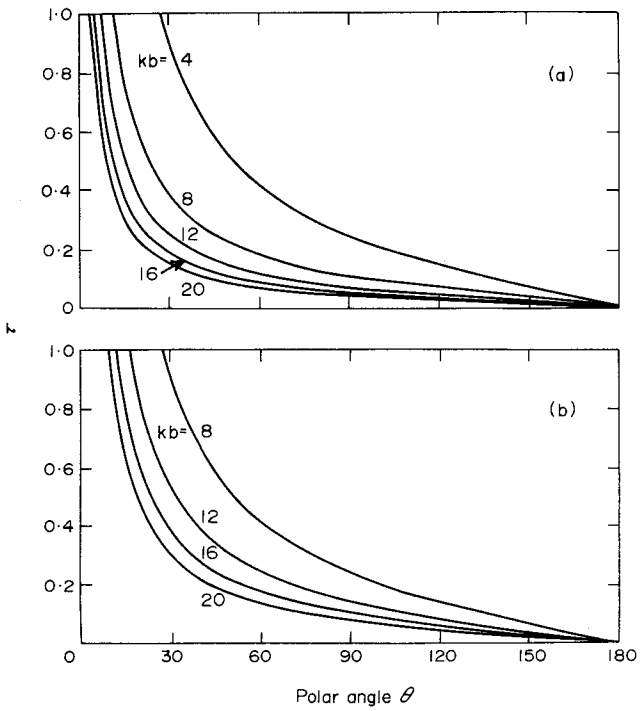

Figure 4. The ratio, τ, of the soft duct far field pressure to the hard duct far field pressure, as a function of polar angle θ, for mode numbers (a) $N = 1$ and (b) $N = 2$.

The soft edge produces (see reference [11], p. 314)

$$\phi_{ds}^0 \sim (2\pi/kr)^{-1/2} \frac{2\cos(\Theta/2)\cos(\theta/2)}{\cos\theta + \cos\Theta} e^{ikr + i\pi/4}, \tag{50}$$

while the hard edge yields ([11], p. 322)

$$\phi_{dh}^0 \sim (2\pi kr)^{-1/2} \frac{2\sin(\Theta/2)\sin(\theta/2)}{\cos\theta + \cos\Theta} e^{ikr + i\pi/4}. \tag{51}$$

Then

$$\phi_{ds}^0/\phi_{dh}^0 \sim \cot(\Theta/2)\cot(\theta/2). \tag{52}$$

The diffracted field corresponding to the soft edge is more prominent in the forward direction; if the incidence angle is superior to $\pi/2$ the diffracted field is reduced by a factor $\cot(\Theta/2)$.

A mode (k, N) in a duct may be represented as a combination of plane waves with an incidence angle given by

$$\Theta = \pi/2 + \arccos(N\pi/2kb). \tag{53}$$

Suppose $N\pi/2kb \ll 1$. Then

$$\cot(\Theta/2) \simeq (1/2)(N\pi/2kb) \tag{54}$$

and $\eta \simeq 1$. Expressions (48) and (52) are then identical. These simple computations show how the acoustical characteristics of the region in the neighborhood of the edge (a few wavelengths) significantly modify the diffracted field.

Until now, only ideally soft walls ($\zeta = 0$) have been considered. A qualitative picture has been obtained of the influence of duct lining on the radiation pattern. It was seen that acoustical lining in an engine nacelle may significantly weaken the side radiation from the duct. As the engines of a commercial aircraft remain nearly horizontal during takeoff, landing, and fly-by operations, the side radiation is important. It is difficult at this point to predict the change in ground noise for a real aircraft. A decrease in loudness would occur only if the radiation pattern for the basic duct without lining does not present a prominent lobe near the duct axis. In any event, a reduction in the duration of maximum loudness can be expected.

Finally, it is worth considering the extension of the method of section 2 to study the radiation from a duct with a real lining (finite impedance) in a uniformly moving medium. For a stationary medium the impedance condition (47) applied at the lining surface. When the medium above the lining flows uniformly, the condition at the absorbing wall changes. At the present time there is some uncertainty concerning the correct condition to apply.

If continuity of displacement at the absorbing material boundary is assumed, as proposed by Ingard [12], this implies that the specific impedance of the material represents the ratio of the pressure to the time derivative of the displacement ξ_t,

$$p/\xi_t = \bar{\rho}c/\beta. \tag{55}$$

The momentum equation in the n direction gives

$$\bar{\rho}\left(\frac{\partial}{\partial t} + \bar{u}\frac{\partial}{\partial x}\right)^2 \xi = -\frac{\partial p}{\partial n}, \tag{56}$$

and together with definition (7) for the incoming modes, yields the new boundary condition:

$$\frac{\partial p}{\partial n} = ik(1 - Mk_x/k)^2 \beta p. \tag{57}$$

If, on the other hand, it is supposed that the material impedance represents the ratio of pressure to normal velocity fluctuations, then, in place of equation (57),

$$\frac{\partial p}{\partial n} = ik(1 - Mk_x/k)\beta p \tag{58}$$

is obtained. In both equations (57) and (58), k_x has the form (20), but because it enters in the boundary condition it is therefore determined by an iterative process; consequently the eigenvalues μ_{mn} of the problem for f will be the solutions of a transcendental equation and will depend on the Mach number of the uniform flow. Therefore, in addition to the transformation, equations (21)–(23), the admittance β for $M = 0$ must be replaced by a new admittance β_1 to take the effect of the uniform flow on the absorbing material into account.

ACKNOWLEDGMENT

The author is grateful to Professor Frank E. Marble for helpful discussion and criticism of the present work.

REFERENCES

1. J. S. B. MATHER, J. SAVIDGE and M. J. FISHER 1971 *Journal of Sound and Vibration* **16**, 407–418. New observations on tone generation in fans.
2. A. H. MARSH, I. EVANS, J. C. HOEHNE and R. L. FRASCA 1968 *National Aeronautics and Space Administration, Washington, D.C.*, CR-1056. A study of turbofan engine compressor noise-suppression techniques.
3. J. M. TYLER and T. G. SOFRIN 1962 *Society of Automotive Engineering Transactions* **70**, 309–332. Axial flow compressor noise studies.
4. R. MANI 1972 Manuscript accepted for publication in *Quarterly of Applied Mathematics*. Refraction of acoustic duct waveguide modes by exhaust jets.
5. S. M. CANDEL 1972 *Journal of Sound and Vibration* **24**, 87–91. Acoustic transmission and reflection by a shear discontinuity separating hot and cold regions.
6. S. M. CANDEL 1972 Submitted for publication in *Journal of the Acoustical Society of America*. Diffraction of a plane wave by a half plane in a subsonic and supersonic medium.
7. B. NOBLE 1958 *Methods Based on the Wiener–Hopf Technique*. New York: Pergamon Press.
8. S. M. CANDEL 1972 *California Institute of Technology, Ph.D. Dissertation, Chapter* 5. Analytical studies of some acoustical problems of jet engines.
9. M. V. LOWSON 1969 *National Aeronautics and Space Administration, Washington, D.C.*, CR-1287. Theoretical studies of compressor noise.
10. R. E. COLLIN 1969 In *Antenna Theory, Part I.* (R. E. Collin and F. T. Zuhker, Eds.). New York: McGraw-Hill Book Company, Inc.
11. J. J. BOWMAN and T. B. A. SENIOR 1969 In *Electromagnetic and Acoustic Scattering by Simple Shapes*. (J. J. Bowman, T. B. A. Senior, and P. L. E. Uslenghi, Eds.). New York: John Wiley and Sons. See Chapter 8.
12. K. U. INGARD 1959 *Journal of the Acoustical Society of America* **31**, 1035–1036. Influence of fluid motion past a plane boundary on sound reflection, absorption and transmission.

APPENDIX I

SIMULATION OF ANNULAR DUCT MODES

The following results are given by Mani [4]; a brief "proof" is added here.

Consider an annular duct of radius r_0, hub to tip ratio σ, and annular spacing $2b$ with

$$b = r_0(1-\sigma)/(1+\sigma). \tag{A1}$$

An acoustic mode propagating in this duct is characterized by the reduced frequency kr_0, and by the radial and tangential mode numbers n and m. The radial mode number is equal to the number of radial pressure nodes, and the tangential mode number is the same as the number of lobes of the pressure pattern.

The wavelength in the tangential direction is $\lambda_\theta = 2\pi r_0/m$ and the tangential wave number is $k_\theta = m/r_0$. The wavenumber in the x-direction, k_x, is given by

$$k_x^2 + k_\theta^2 = k^2, \tag{A2}$$

and thus

$$(k_x b) = kr_0 \frac{1-\sigma}{1+\sigma}\left[1 - \left(\frac{m}{kr_0}\right)^2\right]^{1/2}. \tag{A3}$$

The left-hand side represents the reduced frequency of a mode in a duct formed by two parallel semi-infinite plates set at a distance $2b$ which simulates approximately the annular duct mode. In addition, the mode number N should be taken equal to the radial mode number n to obtain the same number of radial pressure nodes in the two-plate duct.